SUPERHEAVY NUCLEI AND BEYOND: A POSSIBLE UPPER BOUND OF THE PERIODIC TABLE

A. Bhagwat[a], Y.K. Gambhir[b,c], M. Gupta[b]

[a]UM-DAE Centre for Excellence in Basic Sciences, Mumbai 400098, India
[b]Manipal Centre for Natural Sciences, Manipal University
Manipal 576104, Karnataka, India
[c]Department of Physics, IIT-Bombay, Powai, Mumbai 400076, India

(Received March 4, 2016; revised version received May 23, 2016)

Systematic calculations of superheavy region from $Z = 100$ to $Z = 150$ and N/Z ratio ranging from 1.19 to 2.70 have been carried out within the framework of the Relativistic Hartree–Bogolyubov model. It has been shown that the possible upper limit on the periodic table could be $Z = 146$, which is at variance with predictions of sophisticated atomic many-body calculations.

DOI:10.5506/APhysPolB.47.2003

1. Introduction

The question of an upper bound on the possible atomic numbers appearing in the periodic table is an interesting, important but difficult problem, which requires inputs from atomic physics as well as nuclear physics. Using the quantum many-body theory for atomic systems [1, 2], recently, Pyykkö [3] estimated the upper bound to be at charge number $Z = 172$, which is 54 charge numbers away from the highest experimentally known Z, 118 [4]. In the context of finding a possible upper limit on Z, these calculations, though highly sophisticated, should be supplemented by the information about nuclear structure and hence the stability. The present work is an attempt to establish, from the nuclear structure point of view, a possible upper limit on observable value of the charge number. It is, in fact, the interplay between stability of atomic system with given number of electrons and stability of nucleus with given charge number that is finally going to decide on the possible upper limit, if it exists.

Here, we work within the framework of the well-established Relativistic Mean Field/energy density functional, also known as the Effective Mean Field theory [5–9], established to be one of the most successful structure

models that describes ground state properties such as binding energies, radii of the nuclei spanning the entire periodic table. The essentials of the relativistic mean field (RMF) theory are contained in the second section. The results and their discussion form the subject matter of the third section. Summary and conclusions are contained in the fourth section.

2. RMF/RHB calculation and discussion of ground state properties

The starting point for the Relativistic Mean Field theory [5–9] is a Lagrangian density, describing the Dirac spinor nucleons, interacting by exchange of isoscalar–scalar σ meson that simulates long-range attraction, isoscalar–vector ω meson that simulates short-range repulsion, isovector–vector ρ meson that provides the crucial isospin dependence, and the photon for electromagnetic interaction. Here, we use the standard nonlinear interaction Lagrangian with σ self-coupling, which has been used successfully to describe a variety of ground state properties of nuclei spanning the entire periodic table. The Lagrangian density with minimal coupling is composed of the free baryonic ($\mathcal{L}_{\mathcal{B}}^{\text{free}}$), the free mesonic ($\mathcal{L}_{\mathcal{M}}^{\text{free}}$), and the interaction ($\mathcal{L}_{\mathcal{BM}}^{\text{interaction}}$) terms (see, for example, Refs. [7, 8]) such that the net Lagrangian density is given by

$$\mathcal{L} \;=\; \mathcal{L}_{\mathcal{B}}^{\text{free}} \;+\; \mathcal{L}_{\mathcal{M}}^{\text{free}} \;+\; \mathcal{L}_{\mathcal{BM}}^{\text{interaction}} \,. \tag{1}$$

The free baryonic part is given by [7, 8]

$$\mathcal{L}_{\mathcal{B}}^{\text{free}} \;=\; \bar{\psi}_i \left(i\gamma^\mu \partial_\mu \;-\; M\right) \psi_i \,. \tag{2}$$

The free mesonic part, on the other hand, is expressed as [7, 8]

$$\begin{aligned} \mathcal{L}_{\mathcal{M}}^{\text{free}} \;=\; & \tfrac{1}{2}\, \partial^\mu \sigma\, \partial_\mu \sigma - U(\sigma) - \tfrac{1}{4}\, \boldsymbol{\Omega}^{\mu\nu}\; \boldsymbol{\Omega}_{\mu\nu} + \tfrac{1}{2}\, m_\omega^2\, \omega^\mu\, \omega_\mu \\ & - \tfrac{1}{4}\, \vec{\boldsymbol{R}}^{\,\mu\nu}\; \vec{\boldsymbol{R}}_{\mu\nu} + \tfrac{1}{2}\, m_\rho^2\, \vec{\rho}^{\,\mu}\, \vec{\rho}_\mu - \tfrac{1}{4}\, F^{\mu\nu} F_{\mu\nu} \,, \end{aligned} \tag{3}$$

and the interaction term is taken to be [7, 8]

$$\begin{aligned} \mathcal{L}_{\mathcal{BM}}^{\text{interaction}} \;=\; & -g_\sigma\, \bar{\psi}_i \psi_i\, \sigma - g_\omega\, \bar{\psi}_i \gamma^\mu \psi_i\, \omega_\mu - g_\rho\; \bar{\psi}_i \gamma^\mu \vec{\tau} \psi_i\, \vec{\rho}_\mu \\ & - e\, \bar{\psi}_i \gamma^\mu \frac{(1+\tau_3)}{2} \psi_i\; A_\mu \,. \end{aligned} \tag{4}$$

The quantity $U(\sigma)$ contains the σ–σ self-interaction terms, and is given by [14]

$$U(\sigma) = \tfrac{1}{2}\, m_\sigma\, \sigma^2 + \tfrac{1}{3}\, g_2\, \sigma^3 + \tfrac{1}{4}\, g_3\, \sigma^4 \,. \tag{5}$$

In the equations above, M is the nucleon mass, the quantities m_σ, m_ω and m_ρ (g_σ, g_ω and g_ρ) are meson masses (coupling constants), whereas g_2 and g_3 are the coupling constants for the cubic and quartic self-interaction terms for the σ field [14], and e is the electronic charge. The symbol $\vec{\tau}$ (τ_3) denotes isotopic spin (third component of $\vec{\tau}$) for the nucleon spinor (τ_3 is -1 for a neutron and $+1$ for proton). The isovector–vector field $\vec{\rho}^{\,\mu}$ is essential in determining the behaviour of the model with isospin.

The electromagnetic field tensor ($F^{\mu\nu}$) and the field tensors corresponding to the ω and ρ fields ($\boldsymbol{\Omega}^{\mu\nu}$ and $\boldsymbol{R}^{\mu\nu}$) are given by

$$\boldsymbol{\Omega}^{\mu\nu} = \partial^\mu \omega^\nu - \partial^\nu \omega^\mu \,, \tag{6}$$

$$\boldsymbol{R}^{\mu\nu} = \partial^\mu \vec{\rho}^{\,\nu} - \partial^\nu \vec{\rho}^{\,\mu} \,, \tag{7}$$

$$F^{\mu\nu} = \partial^\mu A^\nu - \partial^\nu A^\mu \,. \tag{8}$$

The isovector quantities are indicated by overhead arrows.

The variational principle yields the equations of motion. In the mean field approximation, the meson and the photon fields are not quantised, and are replaced by their expectation values. The time reversal symmetry and charge conservation are then imposed. This then leads to a set of coupled differential equations, namely, *(i)* the Dirac-like equation with potential terms, describing the nucleon dynamics, and *(ii)* Klein–Gordon-like equations with sources involving nucleonic densities, for mesons and the photon. Explicitly, the resulting Dirac equation reads [7, 8]

$$\left(-\iota\boldsymbol{\alpha}\cdot\boldsymbol{\nabla} + \beta\,(M + g_\sigma\sigma) + g_\omega\omega^o + g_\rho\tau_3\rho_3^o + e\frac{1+\tau_3}{2}A^o\right)\psi_i = \epsilon_i\ \psi_i \,, \tag{9}$$

here, σ, ω^o, ρ_3^o and A^o are the meson and electromagnetic fields. Due to time reversal symmetry, the space-like components of ω^μ, $\vec{\rho}^{\,\mu}$ and A^μ vanish, and only the time-like components survive. These are denoted by superscript 'o' above. The meson and electromagnetic fields are determined from the Klein–Gordon equations [7, 8]

$$\left\{-\nabla^2 + m_\sigma^2\right\}\sigma = -g_\sigma\rho_s - g_2\sigma^2 - g_3\sigma^3 \,, \tag{10}$$

$$\left\{-\nabla^2 + m_\omega^2\right\}\omega^o = g_\omega\rho_v \,, \tag{11}$$

$$\left\{-\nabla^2 + m_\rho^2\right\}\rho_3^o = g_\rho\rho_3 \,, \tag{12}$$

$$-\nabla^2 A^o = e\rho_c \,. \tag{13}$$

The source terms (nuclear currents and densities) appearing in the above equations are given by [7]

$$\rho_s = \sum_i n_i\bar{\psi}_i\psi_i \,, \tag{14}$$

$$\rho_v = \sum_i n_i \psi_i^\dagger \psi_i \,, \tag{15}$$

$$\rho_3 = \sum_i n_i \psi_i^\dagger \tau_3 \psi_i \,, \tag{16}$$

$$\rho_c = \sum_i n_i \psi_i^\dagger \left(\frac{1+\tau_3}{2} \right) \psi_i \,. \tag{17}$$

In practical calculations, the sum in these equations is taken only over the positive energy states, which is known as the no-sea approximation (see, for example, [7, 8] for more details). The quantities, n_i, are known as occupation probabilities. In absence of pairing correlations, these are 1 and 0, respectively, for occupied and unoccupied states. Incorporation of pairing correlations leads to mixing of states, thereby resulting in occupation probabilities which differ from 1 and 0.

The pairing correlations can be incorporated by the simple BCS prescription, or self-consistently through the Bogolyubov transforms, leading to the Relativistic Hartree–Bogolyubov (RHB) equations [8, 10–12]

$$\begin{pmatrix} h_{\rm D} - \lambda & \hat{\Delta} \\ -\hat{\Delta}^* & -h_{\rm D}^* + \lambda \end{pmatrix} \begin{pmatrix} U \\ V \end{pmatrix}_k = E_k \begin{pmatrix} U \\ V \end{pmatrix}_k . \tag{18}$$

Here, λ is the Lagrange multiplier, E_k is the quasi-particle energy, and U_k and V_k are normalized four-dimensional Dirac super spinors

$$\int \left(U_k^\dagger U_{k'} + V_k^\dagger V_{k'} \right) = \delta_{kk'} \,; \tag{19}$$

$h_{\rm D}$ is the usual Dirac Hamiltonian (see [8]) given by

$$h_{\rm D} = -\iota \boldsymbol{\alpha} \cdot \boldsymbol{\nabla} + \beta \left(M + g_\sigma \sigma \right) + g_\omega \omega^o + g_\rho \tau_3 \rho_3^o + e \frac{1+\tau_3}{2} A^o \,. \tag{20}$$

The RHB equations comprise of two parts: *(i)* the self-consistent Dirac type field describing long-range particle-hole correlations. This involves the nucleon mass, the σ field and the time-like components of ω and ρ meson fields, in addition to the time-like component of the electromagnetic field; *(ii)* the pairing field describing the particle–particle correlations. The meson and electromagnetic fields are determined self-consistently through the Klein–Gordon-like equations as discussed above. The pairing field is expressed in terms of the matrix elements of a suitable two-body nuclear potential in the particle–particle channel and pairing tensor (Δ). In the case of constant gap approximation, the RHB equations reduce to the usual RMF equations with occupancies given by the usual BCS type of expressions.

In the practical RHB calculations, one needs the parameters appearing in the Lagrangian, as well as the pairing matrix elements. Several sets of these parameters appearing in the Lagrangian are available in the literature [8, 13, 15–22]. In the present work, we employ one of the most widely used Lagrangian parameter sets, NL3 [16].

In absence of any reliable two-body nuclear potential derived within the framework of the RMF model [8, 12], here, we use the finite range Gogny–D1S [23, 24] interaction, which is known to have the right content of pairing. The RHB calculations have been carried out in spherical harmonic oscillator basis. For the purpose of the present exploratory investigations, 20 fermionic and 20 bosonic shells have been found to be adequate. We now present and discuss the principal results of the current investigation.

3. Results and discussion

The RMF/RHB results for the region of known nuclei are found to be in close agreement with the experimental data. The binding energies are found to agree within 0.3% of the experimental values [25, 26], whereas the charge radii are reproduced within 0.5% of the measured values [27]. These observations are very standard, and will not be discussed further.

In order to map the entire superheavy region, all 9377 nuclei with $100 \leq Z \leq 150$ and N/Z ratio ranging from 1.19 to 2.70 have been considered. The entire range has been divided for convenience into two regions: $100 \leq Z \leq 126$ (region 1) and $126 \leq Z \leq 150$ (region 2). The ranges of neutron numbers are taken to be $150 \leq N \leq 260$ and $200 \leq N \leq 350$, respectively. These choices are adequate to cover the neutron as well as proton drip lines for the entire range of Z values. The calculations have been carried out for even–even, even–odd, odd–even as well as odd–odd nuclei.

In the case of the odd–odd, even–odd and odd–even nuclei, the time reversal symmetry is broken due to the presence of odd particle(s). In such cases, the odd particle(s) is (are) assigned to specific state(s), and the rest of the even–even system is treated in the usual way. This is known as blocking, and one needs to incorporate these effects in the calculations. In practice, the identification of level(s) to be blocked is nontrivial, and is usually guided by either the experimental ground states of the neighbouring nuclei or by the theoretically calculated results of the neighbouring even–even nuclei. Note that it is not necessary to consider the blocking effects if the calculations are carried out with all the currents incorporated. However, such calculations are considerably more difficult and time consuming.

In the present work, we explicitly impose the time reversal symmetry, and the blocking effects are taken into account. However, to keep the number of curves within reasonable limit, we shall only display the results for even–even nuclei.

The calculated binding energy per particle (BE/A) for all the even–even nuclei considered here has been presented in Fig. 1. The horizontal line depicted in Fig. 1 stands for BE/A of 6.5 MeV (see the discussion below regarding this particular value). As expected, the BE/A value increases with increasing neutron number, reaches a maximum and then decreases as the neutron number increases further. Interestingly, for a narrow range of neutron numbers, all the elements in a given region turn out to have almost equal BE/A value. Further, with increasing Z, the number of nuclei with BE/A greater than 6.5 MeV decreases, an observation, which will be important for the subsequent discussions.

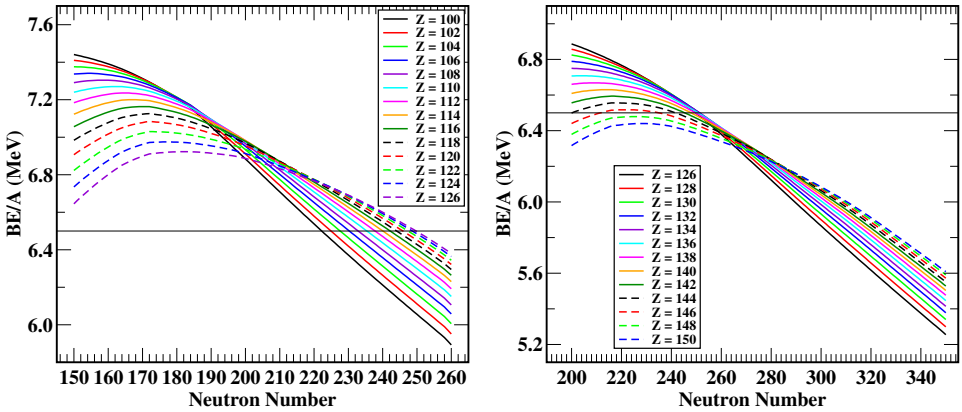

Fig. 1. The calculated binding energy per particle for nuclei with $100 \leq Z \leq 126$ and $126 \leq Z \leq 150$.

As it is well-known, the magicity in the superheavy region depends on both proton as well as neutron numbers (see, for example, [28]). Pairing energies (Tr$\kappa\Delta/2$, here, κ is anomalous density, see [8]) are one of the measures of magicity and hence stability of a given nucleus in comparison with its neighbours. It should, however, be noted merely smallness of pairing energy does not automatically guarantee the existence of the nucleus (see the discussion below).

We plot the calculated neutron pairing energies as a function of neutron number for the two regions in Fig. 2. The neutron pairing energy is found to have sharp peaks at certain values of neutron numbers, indicating enhanced stability there. In some cases, the pairing energy is found to be close to zero, indicating possible existence of magicity at those combinations of neutron and proton numbers. This indicates that particularly in superheavy region, the magicity depends on both proton and neutron numbers, an observation that has been reported elsewhere [28]. In particular, sharp peaks are observed at neutron numbers (N) 164, 172, 184 and 258. At $N = 164$, nuclei

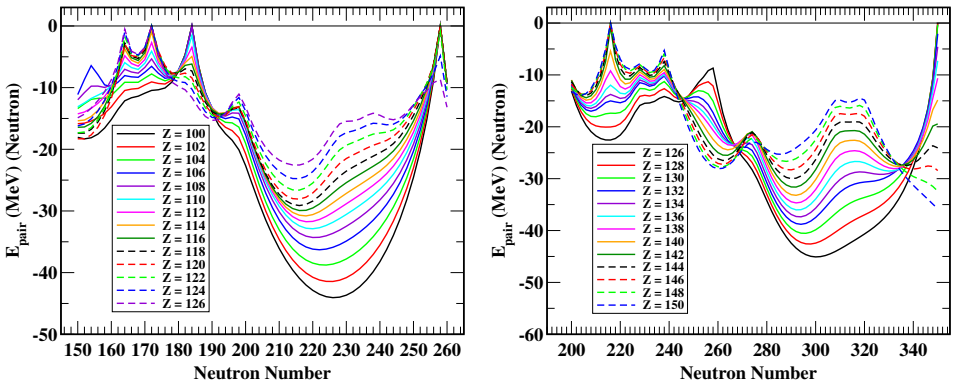

Fig. 2. The calculated neutron pairing energies for region 1 and region 2.

with $Z > 112$ have small neutron pairing energies, but they all are proton unbound, that is, they have positive values of the corresponding proton Fermi energies. On the other hand, at $N = 172$, for the nuclei with $Z > 116$, the neutron pairing energy is very small. The nucleus $^{290}118$ is close to the proton dripline, whereas $^{292}120$ turns out to be just beyond the dripline. Therefore, even if $^{292}120$ turns out to be doubly magic, it is unlikely that it will be observed.

In the case of $N = 184$, nuclei with $Z < 110$ turn out to have very small neutron pairing energy, implying enhanced binding for these cases. All the elements considered in region 1 turn out to have almost zero neutron pairing at $N = 258$. However, all these nuclei turn out to have small BE/A values, consequently, are unlikely to be stable (see the discussion below). In the case of region 2, a robust shell closures exists at neutron number 216, at which, nuclei in the range of $129 \leq Z \leq 141$ are found to be well-bound. On the other hand, the nuclei with very small pairing energy at neutron number 346 either are not bound, or turn out to have small values of BE/A, and are unlikely to survive.

Next, we plot the proton pairing energies for the nuclei appearing in regions 1 and 2 in Fig. 3 as a function of proton number. Each figure has been divided into four panels, each being characterised by an integer, k. For example, the panel with $k = 0$ (region 1) corresponds to neutron numbers from 150 to 176, $k = 1$ corresponds to neutron numbers 178 to 304 and so on. The neutron numbers plotted for region 2 are to be interpreted along the same lines. A close inspection of these figures indicates that there are sharp peaks existing in the graphs, indicating small or nearly zero pairing energies for various charge numbers. The peak in $k = 0$ panel, for $Z = 120$, seems to be robust, and as remarked earlier, the corresponding neutron pairing energy is zero at $N = 172$, making $^{292}120$ a doubly magic nucleus. Unfortunately, this nucleus turns out to be unbound. The charge number

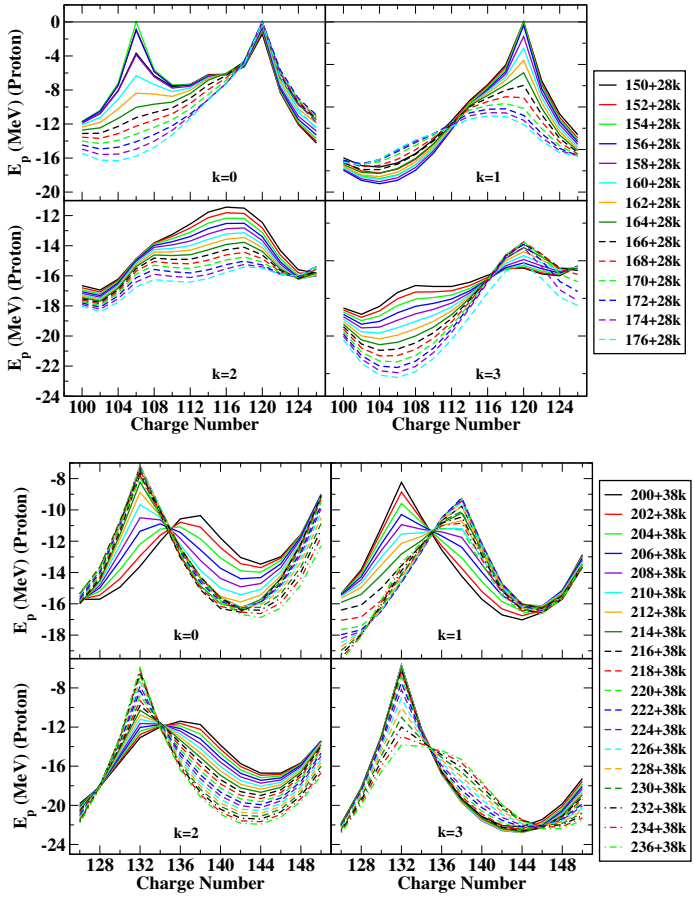

Fig. 3. The calculated proton pairing energies for region 1 and region 2.

106 (Sg) has a few neutron numbers at which proton pairing energy is zero or small. Sg isotopes around these neutron numbers are known, and have been studied experimentally. In the case of $k = 1$, there is one peak at $Z = 120$, but its corresponding neutron pairing energies are large. In the case of region 2, sharp peaks are seen, but in all these cases, the pairing energies are significant (around -6 MeV), and no protonic shell closures are found there. All these observations are consistent with the results discussed in Ref. [28].

The shell closures are reflections of pairing energies. Another measure of shell closures are the separation energies. We next plot two neutron and two proton separation energies for regions 1 and 2 in Figs. 4 and 5, respectively. As expected, the kinks in pairing energies appear at the places, where pairing energy undergoes a sudden change.

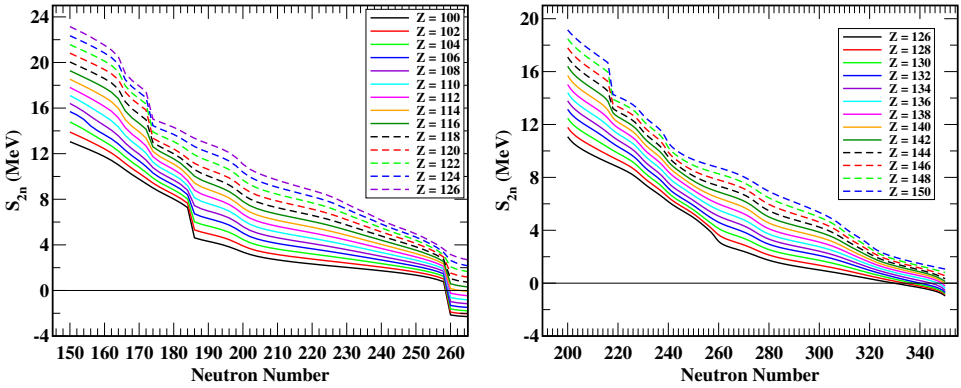

Fig. 4. The calculated two neutron separation energies for region 1 and region 2.

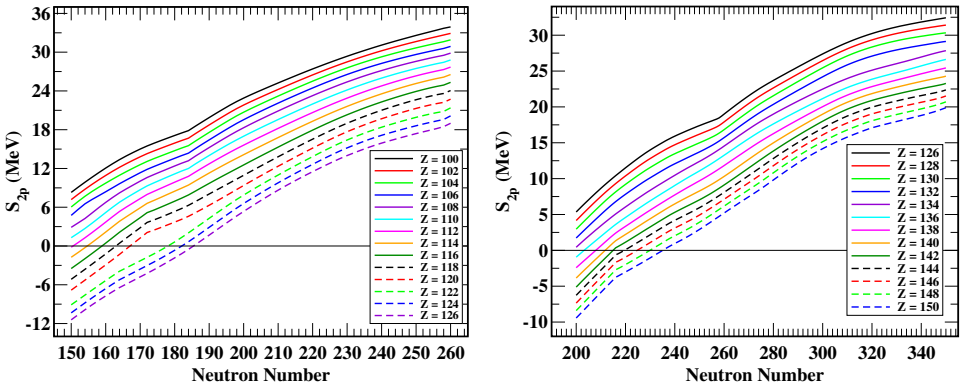

Fig. 5. The calculated two proton separation energies for region 1 and region 2.

Having studied all the 9377 nuclei systematically, we now attempt to answer an important question: how many of these are bound, and even if we do get a bound solution, how many of them are likely to be observed experimentally? To resolve this problem, we first demand that one and two particle separation energies should be positive. This requirement reduced the number of possible nuclei from 9377 to 6507. In this set, the values of BE/A range from $\sim$ 7.5 MeV to $\sim$ 5.3 MeV. In order to understand this range better, we first look at the experimental values of BE/A for the nuclei spanning the entire periodic table.

The binding energy per nucleon (BE/A) of all the known nuclei [25, 26] with $Z \geq 8$ and $N \geq 8$ has been plotted in Fig. 6 as a function of asymmetry parameter ($I = (N-Z)/A$). The graph has been divided into horizontal and vertical sectors, each representing certain range of BE/A or I. The number of nuclei appearing in a given sector are mentioned suitably. For example,

there are 12 nuclei appearing in the range of $-0.2 \leq I \leq -0.1$, and 4 nuclei appearing in the range of $6.4 \leq \mathrm{BE}/A \leq 6.8$ MeV. A close examination of the graph reveals that the most of the known nuclei appear within the range of $0.0 \leq I \leq 0.25$, which is hardly a surprise, and that most of them have their BE/A values larger than 7.4 MeV. In fact, one can also see that the number of nuclei appearing in different BE/A bins goes on decreasing with decreasing BE/A. Hardly four known nuclei have BE/A in the range from 6.4 MeV to 6.8 MeV. These nuclei are ^{20}Mg, ^{25,26}O and ^{28}F.

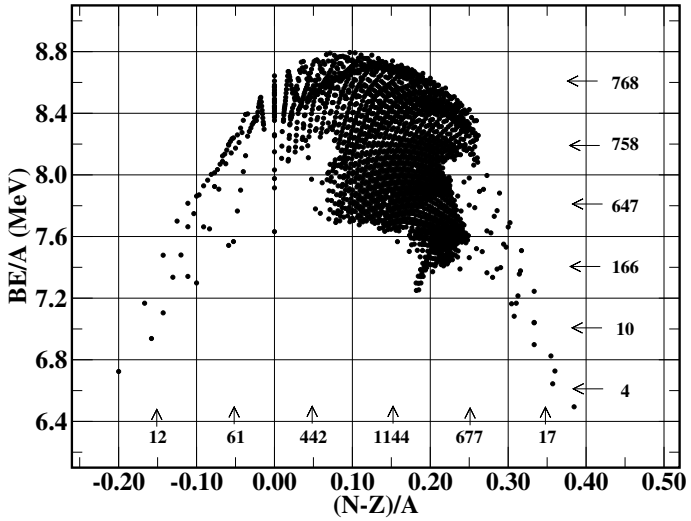

Fig. 6. The experimental [25, 26] binding energy per particle for nuclei with $Z \geq 8$ and $N \leq 8$.

The principal aim of the present work being investigation of stability of the superheavy nuclei, we set a lower cutoff of 6.5 MeV on the calculated BE/A values, considering the discussion on the experimental BE/A above. This reduces the number of possible nuclei from 6507 to 3001, $Z = 146$ being the largest possible Z allowed. We next note that the pairing energy is a measure of degree of shell closure, and hence enhanced stability for the given combination of N and Z values. Among the 3001 surviving the above criterion, it is found that a significant number of nuclei have very large neutron and/or proton pairing energies, and in a number of cases, these values exceed -30 MeV. Clearly, these nuclei are far from shell closure, and are unlikely to be stable. To pin down the number of possible nuclei further, we set a cutoff on pairing energies at -20 MeV. This cutoff is quite conservative, considering the region that we are looking at. With this cutoff, the number of possible nuclei reduces to 2170, with the highest allowed Z being 146. Finally, we impose a constraint on the half-lives against α decay and fission.

We compute the α decay using the modified Viola–Seaborg formula [4, 29]. This formula though fitted for the known superheavy nuclei, works well even far from the known region: we have explicitly verified this by computing the α decay half-lives of nuclei with large Z (> 130) using the double folded α daughter interaction potential within the WKB framework (details of computation can be found in [30]). For example, the log of half-life ($\log T_\alpha$) calculated for $Z = 146$ and $A = 395$ using theoretical Q value (15.357 MeV) turns out to be -4.371 (-4.519) using the WKB framework [30] (the phenomenological Viola–Seaborg formula [4, 29]), which agree very well with each other.

The fission half-lives are estimated by using two recent phenomenological formulas due to Santhosh [31] and Xu [32]. The cutoff on the half-lives thus obtained has been set at 10^{-10} s. With this limit, the number of possible observable nuclei reduces from 2170 to 964, with $Z = 146$ as the highest allowed charge number. Summary of the 964 nuclei allowed after imposing all these constrains is displayed in Table I.

It can be seen from the table that the constrains that we have imposed do not exclude any of the known superheavy nuclei, indicating that the constraints imposed are reasonable. Thus, it seems that the largest allowed value of charge number is 146.

The results discussed so far have been obtained by ignoring deformation effects. We have checked explicitly that the major conclusions drawn here do not change drastically with the inclusion of deformation, an observation that we had reported earlier [28]. Even with inclusion of deformation effects, the largest possible Z is expected to remain at 146. However, it should be noted that the ranges of the allowed values of A could change by a few units. Further, in an extensive calculation, Zhang *et al.* [34] have reported that different RMF parameters, such as, NL3 [16], DD-ME1 [35], PK1 and PK1R [36] predict almost the same general structures in pairing energies. We, therefore, expect that the general conclusions drawn here will not change appreciably due to choice of RMF Lagrangian. The sophisticated atomic many-body calculations reported in the literature indicate that the possible upper bound on the periodic table could be $Z = 172$. We have extended our calculations up to $Z = 180$, and through the analysis discussed above, have not found any evidence for existence of elements above $Z = 146$.

From the experimental point of view, in addition to the analysis presented in this work, a study of the possible reactions leading to the superheavy elements, as well as an estimation of the corresponding production cross sections is also important. An extensive investigation along these lines has been reported elsewhere [37] with predictions for possible reactions to produce the elements with $Z = 119$, 120 as well as unknown heavier isotopes of $Z = 116$ and 118.

TABLE I

Summary of the allowed nuclei. The known nuclei [33] are also mentioned there.

	Range of A			Range of A	
Z	Allowed	Known	Z	Allowed	Known
100	240 to 266	241 to 260	123	306 to 320	
101	242 to 267	245 to 262	124	309 to 323	
102	245 to 269	248 to 264	125	311 to 326	
103	248 to 270	251 to 266	126	314 to 330	
104	250 to 272	253 to 268	127	316 to 333	
105	253 to 273	255 to 270	128	319 to 336	
106	255 to 275	258 to 273	129	321 to 340	
107	257 to 277	260 to 275	130	324 to 343	
108	259 to 279	263 to 277	131	327 to 347	
109	262 to 281	265 to 279	132	330 to 350	
110	264 to 283	267 to 281	133	332 to 354	
111	265 to 285	272 to 283	134	336 to 357	
112	267 to 287	276 to 285	135	339 to 360	
113	269 to 290	278 to 287	136	343 to 364	
114	271 to 293	285 to 289	137	346 to 367	
115	275 to 295	287 to 291	138	349 to 371	
116	278 to 298	289 to 293	139	352 to 374	
117	281 to 301	291 to 294	140	354 to 378	
118	284 to 304		141	357 to 382	
119	287 to 307		142	360 to 385	
120	293 to 310		143	364 to 386	
121	300 to 313		144	367 to 385	
122	303 to 317		145	371 to 384	
			146	374 to 380	

4. Summary and conclusions

In summary, an extensive and systematic RHB calculations for 9377 nuclei with $100 \leq Z \leq 150$ has been carried out, with principal aim to determine a possible upper limit on observable Z. A number of sophisticated atomic many-body calculations have indicated that the largest possible value of Z could be 172. However, as pointed out earlier, these calculations have to be supplemented by the information on the stability of the nucleus. This becomes crucial particularly while determining the possible termination of the periodic table. Through application of a number of criteria for existence and stability, we have demonstrated that the upper limit on periodic table could be charge number 146, beyond which the nuclei are not likely to survive. Our calculations indicate that this estimation will not change even

after inclusion of deformation effects, even though the details, that is, the allowed range of mass numbers for a given charge number, might change by one or two units only.

Authors thank Eva Lindroth and Peter Ring. A.B. acknowledges financial support from DST, the Government of India (grant number DST/INT/SWD/VR/P-04/2014). Part of this work was carried out under the program Dynamics of Weakly Bound Quantum Systems (DWBQS) under FP7-PEOPLE-2010-IRSES (Marie Curie Actions People International Research Staff Exchange Scheme) of the European Union.

REFERENCES

[1] I.P. Grant, *Relativistic Quantum Theory of Atoms and Molecules: Theory and Computation*, Springer, 2007.

[2] M. Barysz, Y. Ishikawa (Eds.), *Relativistic Methods for Chemistry*, Springer, 2010.

[3] P. Pyykkö, *Phys. Chem. Chem. Phys.* **13**, 161 (2011).

[4] Y.Ts. Oganessian, *J. Phys. G: Nucl. Part. Phys.* **34**, R165 (2007) and references cited therein.

[5] J.D. Walecka, *Ann. Phys. (NY)* **83**, 491 (1974).

[6] Y.K. Gambhir, P. Ring, *Pramana* **32**, 389 (1989).

[7] Y.K. Gambhir, P. Ring, A. Thimet, *Ann. Phys. (NY)* **198**, 132 (1990) and references cited therein.

[8] P. Ring, *Prog. Part. Nucl. Phys.* **37**, 193 (1996) and references cited therein.

[9] D. Vretenar, A.V. Afanasjev, G.A. Lalazissis, P. Ring, *Phys. Rep.* **409**, 101 (2005).

[10] J. Meng, P. Ring, *Phys. Rev. Lett.* **77**, 3963 (1996).

[11] J. Meng, *Nucl. Phys. A* **635**, 3 (1998).

[12] H. Kucharek, P. Ring, *Z. Phys. A* **339**, 23 (1991).

[13] G.A. Lalazissis, P. Ring, D. Vretenar, *Extended Density Functionals in Nuclear Structure Physics*, *Lect. Notes Phys.* **641**, Springer, 2004 and references cited therein.

[14] J. Boguta, A.R. Bodmer, *Nucl. Phys. A* **292**, 413 (1977).

[15] M. Bender, P.H. Heenen, P.-G. Reinhardt, *Rev. Mod. Phys.* **75**, 121 (2003).

[16] G.A. Lalazissis, J. König, P. Ring, *Phys. Rev. C* **55**, 540 (1997).

[17] P.-G. Reinhard *et al.*, *Z. Phys. A* **323**, 13 (1986).

[18] P.-G. Reinhard, *Rep. Prog. Phys.* **52**, 439 (1989).

[19] M.M. Sharma, M.A. Nagarajan, P. Ring, *Phys. Lett. B* **312**, 377 (1993).

[20] M. Bender, W. Nazarewicz, P.-G. Reinhard, *Phys. Lett. B* **515**, 42 (2001).

[21] T. Nikšić, D. Vretenar, P. Ring, *Prog. Part. Nucl. Phys.* **66**, 519 (2011) and references cited therein.

[22] S.E. Agbemava, A.V. Afanasjev, D. Ray, P. Ring, *Phys. Rev. C* **89**, 054320 (2014).

[23] J.F. Berger, M. Girod, D. Gogny, *Nucl. Phys. A* **428**, 23 (1984).

[24] T. Gonzalez-Llarena, J.L. Egido, G.A. Lalazissis, P. Ring, *Phys. Lett. B* **379**, 13 (1996).

[25] G. Audi *et al.*, *Chin. Phys. C* **36**, 1287 (2012).

[26] M. Wang *et al.*, *Chin. Phys. C* **36**, 1603 (2012).

[27] I. Angeli, K.P. Marinova, *At. Data Nucl. Data Tables* **99**, 69 (2013).

[28] A. Bhagwat, Y.K. Gambhir, *Int. J. Mod. Phys. E* **20**, 1663 (2011).

[29] R. Smolańczuk, *Phys. Rev. C* **56**, 812 (1997).

[30] Y.K. Gambhir, A. Bhagwat, M. Gupta, *Ann. Phys. (NY)* **320**, 429 (2005).

[31] K.P. Santhosh, R.K. Biju, S. Sahadevan, *Nucl. Phys. A* **832**, 220 (2010).

[32] C. Xu, Z. Ren, Y. Guo, *Phys. Rev. C* **78**, 044329 (2008).

[33] J.K. Tuli, *Nuclear Wallet Cards*, National Nuclear Data Center, 2011.

[34] W. Zhang *et al.*, *Nucl. Phys. A* **753**, 106 (2005).

[35] T. Nikšić, D. Vretenar, P. Finelli, P. Ring, *Phys. Rev. C* **66**, 024306 (2002).

[36] W. Long, J. Meng, N. van Giai, S.-G. Zhou, *Phys. Rev. C* **69**, 034319 (2004).

[37] H.M. Devaraja, Y.K. Gambhir, M. Gupta, G. Münzengerg, *Phys. Rev. C* **93**, 034621 (2016).